

16 Aug 2008, 8:45am - 12:30pm

Considerations on Different Features of Local Seismic Effect Numerical Simulations: The Case Studied of Castelnuovo Garfagnana

Savino Russo
Technical University of Bari, Bari, Italy

Giovanna Vessia
Technical University of Bari, Bari, Italy

Claudio Cherubini
Technical University of Bari, Bari, Italy

Follow this and additional works at: <https://scholarsmine.mst.edu/icchge>



Part of the [Geotechnical Engineering Commons](#)

Recommended Citation

Russo, Savino; Vessia, Giovanna; and Cherubini, Claudio, "Considerations on Different Features of Local Seismic Effect Numerical Simulations: The Case Studied of Castelnuovo Garfagnana" (2008). *International Conference on Case Histories in Geotechnical Engineering. 2.* <https://scholarsmine.mst.edu/icchge/6icchge/session03/2>

This Article - Conference proceedings is brought to you for free and open access by Scholars' Mine. It has been accepted for inclusion in International Conference on Case Histories in Geotechnical Engineering by an authorized administrator of Scholars' Mine. This work is protected by U. S. Copyright Law. Unauthorized use including reproduction for redistribution requires the permission of the copyright holder. For more information, please contact scholarsmine@mst.edu.



CONSIDERATIONS ON DIFFERENT FEATURES OF LOCAL SEISMIC EFFECT NUMERICAL SIMULATIONS: THE CASE STUDIED OF CASTELNUOVO GARFAGNANA

Dott. Ing. Savino Russo
Technical University of Bari
70125 Bari

Dott. Ing. Giovanna Vessia
Technical University of Bari
70125 Bari

Prof. Ing. Claudio Cherubini
Technical University of Bari
70125 Bari

ABSTRACT

Numerical studies of local seismic effects are commonly carried out by means of 1D and 2D simulations performed in order to evaluate amplification effects in terms of acceleration response spectra and amplification factors. Such approaches can be easily compared with prescriptions from technical provisions as Eurocode 8 that lead design activity whenever a poor soil characterization is available. When suitable investigation campaigns and regional hazard studies are undertaken accurate studies on local seismic effects can be developed. As a matter of fact, soil high heterogeneity and variability, input motion features and geometrical irregularities of soil layer boundaries heavily affect seismic soil response and frequently cause different damages in urban areas. For that reason, although just from deterministic standpoint, spatial variation of amplification effects has been investigated in order to understand how much numerical simulation experiences in amplification provisions can improve simplified approaches suggested by technical codes. In this study Castelnuovo Garfagnana town (Italy) has been studied by means of numerical simulation. Results have been discussed focusing on those aspects which mainly interpret the physical phenomenon that mostly affect seismic local amplification effects.

INTRODUCTION

Over the past ten years, the consequences of seismic events of low to medium intensity level has pointed out that several Italian urban centres are highly vulnerable to seismic local amplification effects. The first attempt of addressing this issue was made in 2003 by means of Law OPCM 3274. It introduces a new seismic zonation in terms of PGA values and several new provisions for buildings in order to lead the Italian building codes toward Eurocode 8. A new sensitivity to seismic microzonation has occurred, and a few Italian Regional Offices have been promoting scientific surveys within urban areas of those towns where building heritage and human lives would be mostly affected by earthquakes. Among others, the Tuscany Region, by means its Seismic Prevention Office, has conducted microzonation studies since 1998 when the VEL project (Evaluation of Seismic Local Effect) was started. The areas investigated are within Lunigiana and Garfagnana counties where the highest seismic hazard level is recorded in the Tuscany Region (Fig. 1). Some districts as Fivizzano, Molazzana, Castelnuovo Garfagnana, were investigated by in situ and laboratory experimental campaigns in order to improve the knowledge of the surficial deposits and simulating their seismic response.

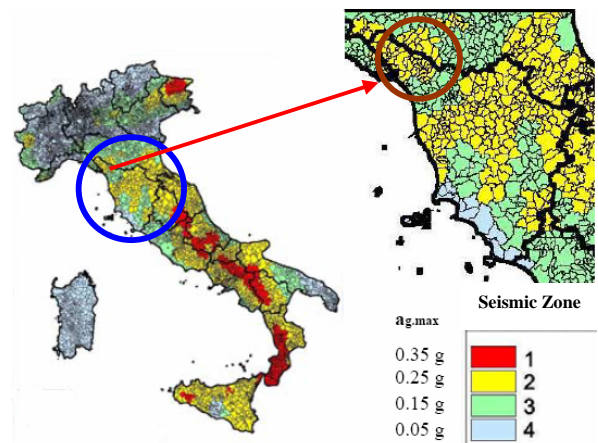


Fig. 1. Updated seismic microzonation of Italian territory (O.P.C.M. n.3274, 2003 and T.U., 2005).

This study is focused on Castelnuovo Garfagnana town and especially on that part of the urban area close to the valley of Serchio river (Fig. 2). This town was investigated by researchers (Lo Presti et al. 2002, Crespellani et al. 2002a, Crespellani et al. 2002b) to evaluate local seismic amplification effect using geophysical and geotechnical field and laboratory tests (Lo Presti et al. 2002).

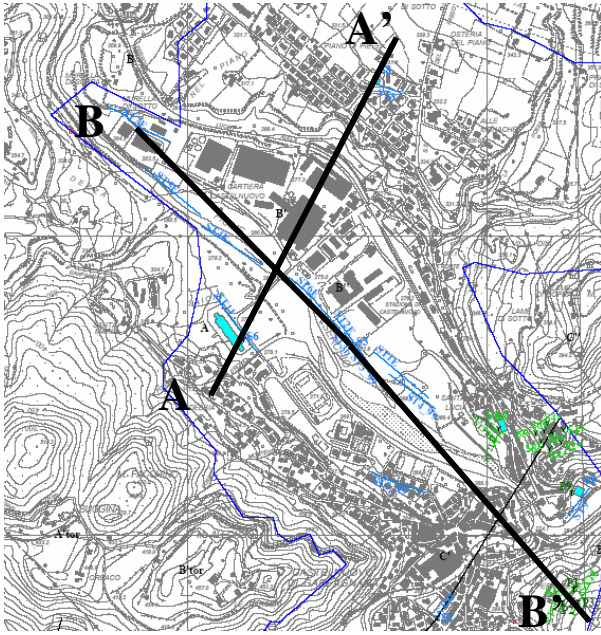


Fig. 2. The two sections AA' e BB' used for numerical analyses of local seismic response and traces of geophysical refraction in situ tests.

Recently, further in situ surveys, consisting on geotechnical and geophysical investigations, have been performed in order to construct other geological-lithological sections and to conduct 1D and 2D numerical simulations. Probabilistic seismic hazard analyses have been carried out by Lai et al. (2005) to develop a new estimation of seismic hazard at Lunigiana and Garfagnana areas according to probabilistic methodology and worldwide earthquake databases. This study provided seven sets of natural accelerograms for each return period: 75, 475 and 2475. For this study a 475 years return period is considered. The present paper summarizes results from improved local seismic response numerical simulations for two sections of Castelnuovo Garfagnana urban area. The main purposes of this study are:

- 1) to show the influence of input motions, soil heterogeneity and geometrical irregularities of layer boundaries on local effects;
- 2) to discuss the best way to estimate amplification factors;
- 3) to suggest the use, in simplified approaches, of stratigraphic and geometrical amplification factors.

CASTELNUOVO GARFAGNANA SITE

Geological, lithological and seismic features

The main geological features of surficial deposits on which Castelnuovo Garfagnana town is located (Cancelli et al. 2002, Nardi et al. 1986, Ferrini et al., 2001) from bottom to the surface consist of:

1. Tuscany sequence represented by “Macigno” sandstone (referred as MG);
2. Ottone-Santo Stefano unit, made up of “M. Penna-Casanova” complex and “Flysh ad Elmintoidi” formation (referred as FH);
3. Villafranchiani deposits made up of mainly clayey-sandy deposits (referred as ARG) covered by clayey-conglomerate sediments (CG);
4. Recent covering soils, which are made up of alluvial deposits from paleo-valleys (PALL) and terraces (AT), recent to present alluvial deposits (ALL), detritals (DT), sliding and covering soils (RP).

In Castelnuovo Garfagnana site three main lithological units, starting from the bottom, are:

- a substratum which is made up of the Macigno sandstone. It is characterized by middle-low mechanical strength and dense to high dense fractures and open joints from 1 to 5 mm. The substratum depth varies from 6 to 10 m whereas nearby Serchio river valley it is more than 10 m depth.
- Villafranchiani deposits which include conglomerate with clusters locally cemented and stiff clays.
- Covering soils which are recent alluvial deposits that can be classified from moderately dense to loose soils with sandy or clayey fractions.

According to the present Italian seismic classification, Castelnuovo Garfagnana town is classified as zone 2 where the outcropping maximum expected PGA equals 0.25g. Since 1740 this town, which has a valuable historical heritage, has been struck by numerous strong earthquake summarized in Table 1.

Table 1. Past significant seismic events in Garfagnana area (Cancelli et al., 2002).

Date	Intensity (M.C.S.)	Epicentral zone
6-3-1740	VIII-IX	Barga
19/23-7-1746	VIII	Barga
11-4-1837	IX	Alpi Apuane
10-6-1904	VIII	Appennino Modenese
7-9-1920	IX-X	Villa Collemantina
10-12-1937	VII	Appennino Modenese
15-10-1939	VII	Alpi Apuane
23-1-1985	VI	Garfagnana
10-2-1987	VI	Giuncugnano

Past microzonation experiences

Past studies have been carried to simulate seismic response of surficial deposits. Dynamic characterization was conducted by geological, geophysical and geotechnical investigations (Cancelli et al. 2002, Foti et al. 2002), and numerical simulations were carried out by Lo Presti et al. (2000) and Lo Presti et al. (2002). Numerical analyses were performed using two 1D numerical codes: Shake91 (Idriss and Sun 1992) and

Onda (Lo Presti et al. 2001) and a 2D code Quad4M (Hudson et al. 1994). The input motions used were synthetic accelerograms calculated by Petrini (1998). Results were presented as acceleration spectra from 1D and 2D numerical simulations (Pergalani et al., 1999; Bouckovalas et al., 1999). Lo Presti et al. (2002) used two different formulations for computing amplification factor. The amplification factor from Pergalani et al. (1999) is defined below:

$$Fa = \frac{\int_{0.1}^{0.5} PSV(T, \xi) dT_{(out)}}{\int_{0.1}^{0.5} PSV(T, \xi) dT_{(input)}} \quad (1)$$

where PSV is the pseudo-velocity spectrum, and 0.1 to 0.5 s represents the range of periods for measuring amplification effects both for 1D and 2D analyses. Topographic amplification coefficients were investigated, according to Bouckovalas et al. (1999):

$$f_{S_a} = \frac{S_a(T, 2D)}{S_a(T, 1D)} \quad (2)$$

where S_a is the acceleration spectra from 2D and 1D analyses calculated at $T = 0.2$ s or $T = 0.4$ s. This factor measures amplification effects due to surficial geometrical irregularities. These analyses present amplification factors at Castelnuovo Garfagnana site without discussing a more general use in engineering designing activity.

Present study

For the present study new investigations located within the urban centre of Castelnuovo Garfagnana town were performed: 6 down holes and 14 seismic refraction tests. Figure 2 shows the experimental test locations and the two sections, AA and BB, used for 1D and 2D numerical simulations. Figures 3 and 4 illustrate the models of the two sections studied below. Lithotypes are reported in Fig. 3 and Fig. 4 according to the acronyms explained in Table 2.

Table 2. Lithotypes and their acronyms introduced within Fig. 3 and Fig. 4.

Acronym	Lithotype description	Lithotype name
b ₁	Alluvial deposits, sands and silty loose sands, dense detrital layers, gravels and sands.	Alluvium
AFB	Clays, sandy clays, sands with interbedded pebbles, overconsolidated stiff sands.	Clay
h _n	Soft soil.	Soft soil
MAC	Intact Macigno sandstone.	Bedrock

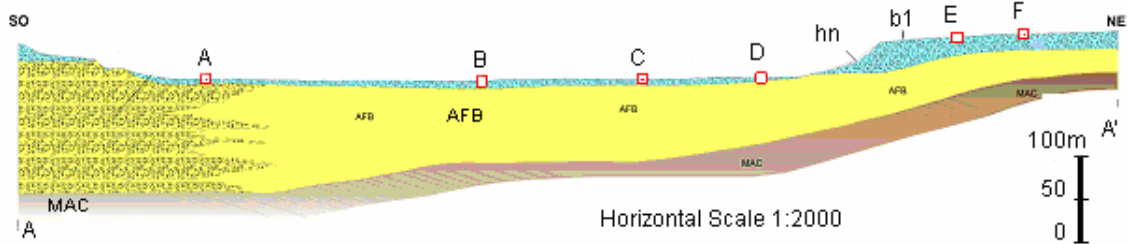


Fig. 3. Lithological section AA'.

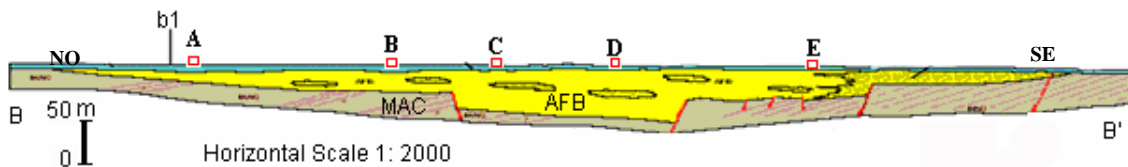


Fig. 4. Lithological section BB'.

Input motion. A probabilistic seismic hazard study was carried out by Lai et al. (2005) for Garfagnana and Lunigiana areas. For the return period of 475 years seven sets of natural accelerograms were developed which are spectrum compatible according to Italian seismic codes. Among them three accelerograms have been employed in this study. They are chosen by considering different duration, frequency content, and energy content of the ground motions. These three accelerograms are called 854X, 642Y and 1320 and their main features are shown in Table 3 and in Figs. 5-7. These input motions, for numerical simulation purposes, have been scaled at Castelnuovo Garfagnana expected acceleration, that is 0.191g and afterwards reduced to a bedrock depth by means of deconvolution. The three input motions are applied as horizontal acceleration time histories. Vertical component were not considered in the present study.

Table 3. Input accelerograms employed in this study.

Code	Earthquake	M _b	M _L	M _s	M _w
854X	Umbro-Marchigiano	5.1	5.2	4.8	5.1
642Y	Umbro-Marchigiano	5.3	5.5	5.6	5.6
1320	Coyote lake	-	5.7	5.6	5.7

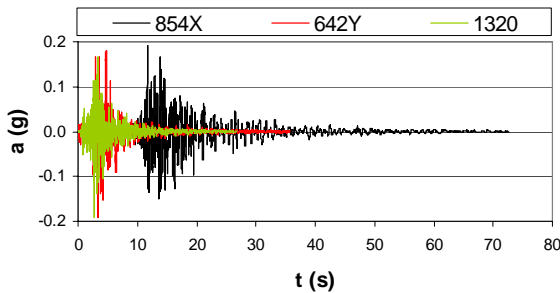


Fig. 5. Time histories of the three input accelerograms.

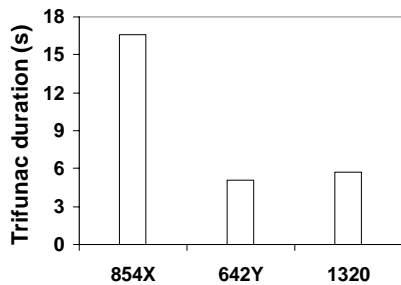


Fig. 6. Trifunac duration of the three input accelerograms.

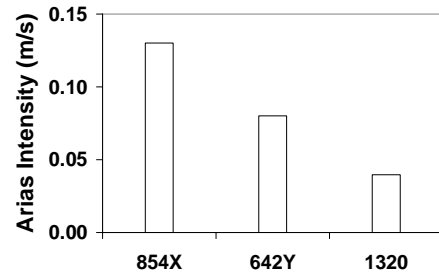


Fig. 7. Arias intensity of the three input accelerograms.

Main features of numerical analyses. The two sections (Figs. 3-4) have been represented in 2D numerical models with triangular constant finite elements whose boundaries follow the rule below:

$$l \leq \frac{V_{SH}}{K \cdot f_{max}} \quad (3)$$

where l is the edge, V_{SH} is the shear wave velocity of the soil types, K is a dimensionless coefficient varying between 6 and 8, and f_{max} is the maximum frequency of the input motion that can be propagated. The 1D and 2D numerical simulations were performed at the 6 and 5 nodes shown (Figs. 3-4) in section AA' and BB' respectively. ProShake code for 1D analyses and Quake module (Gestudio, 2004) for 2D analyses have been used. These codes implement equivalent linear constitutive soil model for soil response analyses. The equivalent linear assumption on seismic soil behaviour was verified by back analysis. The strain level along the sections have been compared with the volumetric thresholds γ_v for each lithotypes to verify that strain values, at control points, are less than volumetric thresholds.

Seismic refraction and down hole tests provided V_{SH} and V_P values along the two sections within each lithotypes as Table 4-7 show. At the bottom of each table mean values (μ), standard deviations (σ) and coefficients of variation (CV) are summarized. The use of average values for each formation in section AA' and BB' is due to the nearly constant V_{SH} measurements for each formation along each down hole.

Despite the high coefficients of variation the influence of soil variability is not critical. Simulations carried out, where local V_{SH} and V_P values were used. Accordingly, in the following discussion only mean values of V_{SH} , density ρ and Poisson ratio ν for each lithotype summarized in table 8 have been used as.

For the case of Macigno formation (see Table 7), the mean value of 900m/s has been used (instead of 940m/s); this value corresponds to an intermediate value between intact and fractured rock. The Macigno formation has been considered as the bedrock, and it has been modelled by linear elastic behaviour.

Table 4. V_{SH} and V_P values measured by geophysical tests for alluvial deposits.

Soil type	ID Test	V_S (m/s)	V_P (m/s)
ALLUVIUM	ST3B	280	933
	STS1	328	593
	ST1T	570	755
	ST2T	108	265
	ST2T	318	1020
	ST3T	98	150
	ST3T	360	660
	ST5	170	393
	ST5	233	923
	ST6	223	460
	ST6	318	763
	ST7	271	546
	ST11	508	1486
	DHS1	393	759
	DHS2	178	311
	DHS3	350	604
	DH6	207	366
	μ	289	646
σ	128	330	
CV (%)	44	51	

Table 5. V_{SH} and V_P values measured by geophysical tests for soft soils.

Soil type	ID Test	V_S (m/s)	V_P (m/s)
SOFT SOIL	ST1F	215	313
	ST2F	180	275
	ST15	142	320
	μ	179	303
	σ	37	24
	CV (%)	20	8

Table 6. V_{SH} and V_P values measured by geophysical tests for clay deposits.

Soil type	ID Test	V_S (m/s)	V_P (m/s)
CLAY	ST3B	833	2467
	ST5	930	2745
	ST6	683	2355
	ST7	445	2100
	ST8	817	2260
	ST11	815	2530
	DHS2	763	1990
	DHS3	818	2081
	DH6	723	2345
	DH8	721	1951
	μ	755	2282
	σ	130	256
	CV (%)	17	11

Table 7. V_{SH} and V_P values measured by geophysical tests for bedrock formation.

Soil type	ID Test	V_S (m/s)	V_P (m/s)
MACIGNO	ST1F	943	3200
	ST2F	1175	2955
	ST9	1121	3003
	ST15	957	2525
	DHS1	717	2193
	DH1F	718	2027
	μ	938	2650
	σ	194	476
	CV (%)	21	18

Table 8. Density, shear wave velocity and Poisson's Ratio values used within numerical simulations of AA and BB sections.

Soil type	Values used for numerical simulations		
	ρ (kg/m ³)	V_s (m/s)	ν
Soft soil	1800	180	0.27
Alluvium	1800	290	0.30
Clay	2100	750	0.45
Bedrock	2500	900	0.35

When performing site response analyses, $G(\gamma)/G_0$ and $D(\gamma)$ curves were defined for each lithotype by means of laboratory cyclic tests. Resonant column and torsional shear tests have been performed (Foti et al., 2002) on undisturbed samples taken from borings (Table 9). These curves were used in subsequent numerical analyses.

Table 9. $G(\gamma)/G_0$ and $D(\gamma)$ curves for each lithotypes from sections AA and BB.

γ (%)	Alluvium		Clay		Soft soil	
	G/G ₀	D (%)	G/G ₀	D (%)	G/G ₀	D (%)
0.0001	1		1	1	0.98	0.95
0.001	0.98	1.4	1	1	0.95	1.5
0.01	0.56	3.8	0.64	1	0.78	3.9
0.03	0.34	7.0	0.40	2	0.60	6.5
0.1	0.16	11.8	0.18	11	0.38	10.8

Seismic amplification factor. In this study an evaluation of seismic amplification effects for geometrical S_g and stratigraphic factors S_s along the two studied sections was performed.

According to Eurocode 8 foundation soil type is defined on the basis of the V_{S30} parameter. Eurocode defines the total

amplification factor S as the product between the stratigraphic factor which depends on foundation soil type and constant topographic factor S_T considered whenever slopes are steeper than 15° . Eurocode 8 doesn't take into account the influence of buried geometrical irregularities and the dependence on the periods of amplification factors.

In the case of Castelnuovo Garfagnana urban area V_{S30} values were calculated along the two sections AA' and BB' at surficial nodes shown Fig. 3-4. Results are illustrated in Table 10. As can be seen almost all of the points belong to the B soil category and the remainder to the C soil category. The amplification factors are required by Eurocode 8 whenever soil seismic response studies are not performed. These values for B and C soil are 1.2 and 1.15 respectively. In order to take into account topographic amplification effects at node E in section AA', which is near a slope higher than 15° , a constant value for topographic amplification factor equals to 1.2 was applied.

Table 10. V_{S30} calculated along section AA' and BB'.

Section AA'						
Point	A	B	C	D	E	F
V_{S30} (m/s)	570	500	540	600	340	360
Soil Category	B	B	B	B	C	C
Section BB'						
Point	A	B	C	D	E	
V_{S30} (m/s)	410	410	490	550	540	
Soil Category	B	B	B	B	B	

Table 11. Reference values of amplification factor from Eurocode 8.

Amplification factors (EC8)	Soil category (EC8)				
	A	B	C	D	E
S_s	1.00	1.20	1.15	1.35	1.40
$S_T(\text{slope} > 15^\circ)$	1.20	1.20	1.20	1.20	1.20
$S = S_s S_T$	1.20	1.44	1.38	1.62	1.68

In the case studied, point E in section AA' belongs to C soil category. The total amplification factor S is equal to (see Tab. 11):

$$S = S_T \cdot S_s = 1.38 \quad (4)$$

For the remaining points, belonging to B and C soil categories, only stratigraphic amplification should be considered, so that:

$$S = S_T = 1.2 \text{ for B soil category}$$

$$S = S_T = 1.15 \text{ for C soil category}$$

From this seismic response study, the total amplification factor S from 2D numerical analyses has been define according to the expression below (Housner 1952, Pergalani et. al. 1999):

$$FA(T = 0.1 - 2.5s) = \frac{\int_{0.1}^{2.5} [\text{PSV}(T, \xi = 5\%)]_{\text{out}} dT}{\int_{0.1}^{2.5} [\text{PSV}(T, \xi = 5\%)]_{\text{inp}} dT} \quad (5)$$

where PSV is the pseudo-velocity spectrum integrated on a range of periods 0.1 s to 2.5 s. The same expression has been used to evaluate the stratigraphic amplification factor S_s from 1D analyses. The 2D numerical simulations consider the effects of soil layer sequences and both surficial and buried geometrical irregularities, whereas 1D simulations allow us to take into account the effects of layer sequences.

The topographic amplification factor has been calculated as the ratio between 2D and 1D acceleration response spectra at two periods, that is $T = 0.2$ s and $T = 0.4$ s according to Bouckovalas et al. (1999) definition:

$$f_a = \frac{S_a^{(2D)}(T)}{S_a^{(1D)}(T)} \quad (6)$$

Results from numerical analyses. Results from 2D analyses are provided at surficial nodes shown in Figs. 3-4. They consist of acceleration response spectra (for 5% damping), stratigraphic amplification factors according to Eq. (5) applied to 1D results and topographic amplification factors according to Eq. (6).

For preliminary analyses, soil heterogeneity was taken into account in 2D simulations (local values of V_{SH} , $G(\gamma)/G_0$ and $D(\gamma)$) for each input motion. A comparison of results, show that the most relevant differences are associated with the input motion records. Therefore, results presented are for to mean values of soil properties and three different input motions taken from probabilistic seismic hazard analysis.

The 2D acceleration response spectra are reported in Figs. 8a-b and 9a-c. Figures 8a-c show results from section AA' and Figs. 9a-c from section BB'. The letters a-c refer to the three input motions used.

As can be observed, the 2D analyses in both sections show amplification effects over a range of periods from 0.15 s to 0.9 s for 854X and 642Y input motions. For these input motions the highest S_a values are at A, B and C nodes in section AA', and they are due to the thickness of both clayey deposits and the overlying alluvial layer. The shape of these spectra shows high peaks varying from 1.2g to 2g associated with the natural periods of the soil column.

Nodes E and F show the filtering effects of thick alluvial deposits (about 20m), whereas node D is mostly affected by the bedrock shape.

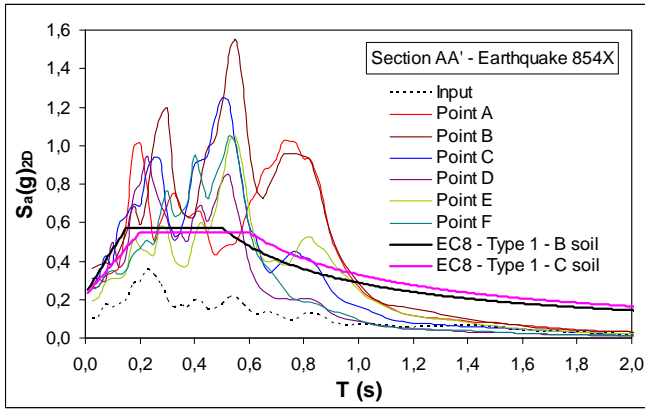


Fig. 8a. Comparison between acceleration response spectra calculated by means of 2D simulations and Eurocode 8 response spectrum for section AA' and input motion 854X.

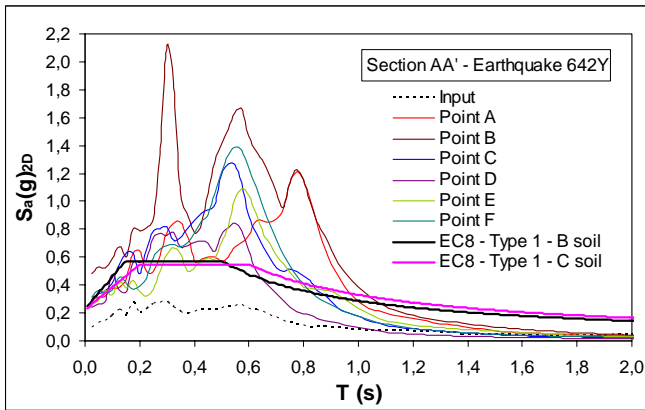


Fig. 8b. Comparison between acceleration response spectra calculated by means of 2D simulations and Eurocode 8 response spectrum for section AA' and input motion 642Y.

For section BB' and for input motions 854X and 642Y, the more irregular the bedrock shape the more the acceleration spectral values S_a . This phenomenon is particularly relevant near the node C, D and E where S_a values vary from 1.4g and 4g.

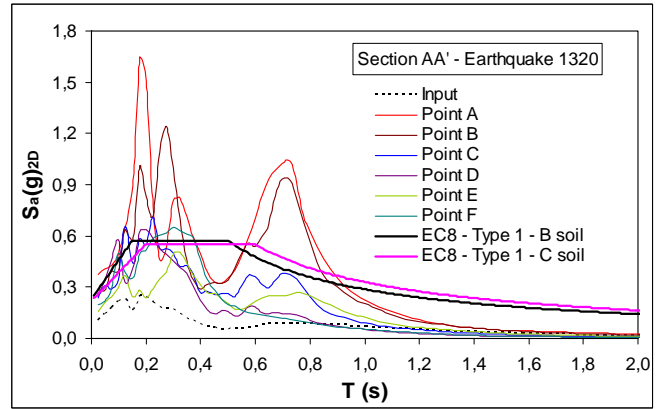


Fig. 8c. Comparison between acceleration response spectra calculated by means of 2D simulations and Eurocode 8 response spectrum for section AA' and input motion 1320.

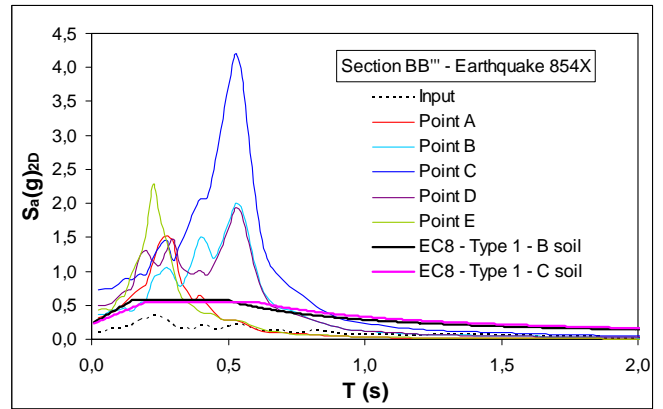


Fig. 9a. Comparison between acceleration response spectra calculated by means of 2D simulations and Eurocode 8 response spectrum for section BB' and input motion 854X.

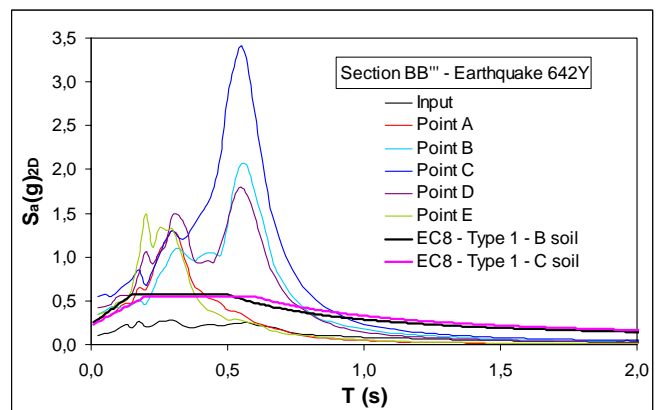


Fig. 9b. Comparison between acceleration response spectra calculated by means of 2D simulations and Eurocode 8 response spectrum for section BB' and input motion 642Y.

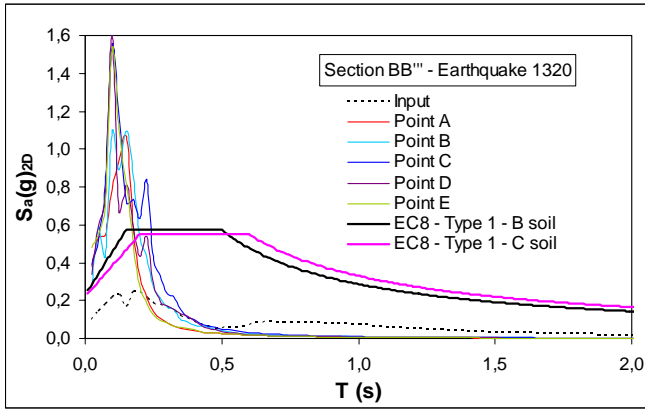


Fig. 9c. Comparison between acceleration response spectra calculated by means of 2D simulations and Eurocode 8 response spectrum for section BB' and input motion 1320.

Similar spectral shapes have been shown for sections AA' and BB' for 854X and 642Y input motions.

In the case of the 1320 accelerogram the amplification effect along section BB' has a narrower range of periods from 0.05 s to 0.2 s. In section AA' two ranges of periods are amplified, that is 0.15 s to 0.3 s and 0.6 s to 0.85 s. This response can be due to the frequency content of the 1320 acceleration Fourier spectrum that shows its predominant period at about 0.2 s while for 642Y and 854X input motions the predominant periods are 0.6 s and 0.4 s.

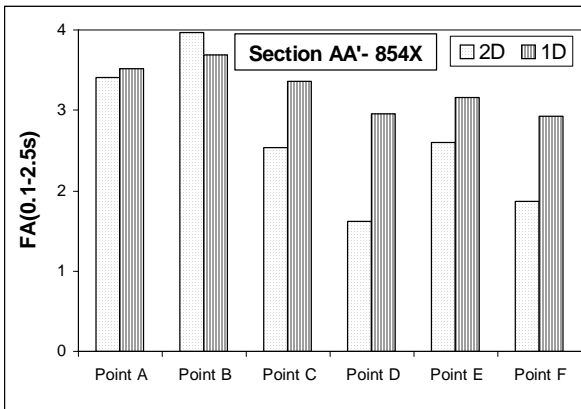


Fig. 10a. Amplification factors corresponding to 6 surficial points on section AA' for 854X input motion.

The 1D results in terms of acceleration spectra (not reported here) show ranges of periods are amplified: 0.2 s to 0.4 s and 0.5 s to 0.9 s. This is true for the 854X and 642Y input motions and for sections AA' and BB'. In the case of the 1320 accelerogram, two different ranges of periods are amplified: 0.05 s to 0.3 s and 0.6 s to 0.85 s.

Total amplification factors S from 2D and stratigraphic amplification factor S_s from 1D analyses, according to Eq. (5)

were calculated for section AA' (Fig. 10a-c) and section BB' (Fig. 11a-c) for the three input accelerograms.

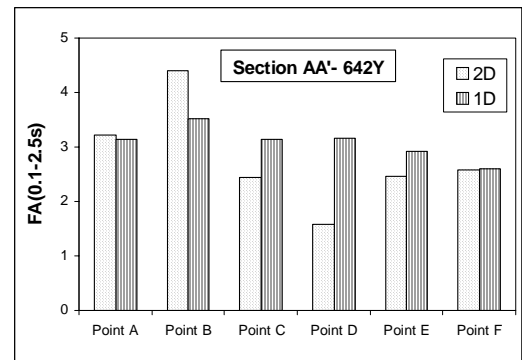


Fig. 10b. Amplification factors corresponding to 6 surficial points on section AA' for 642Y input motion.

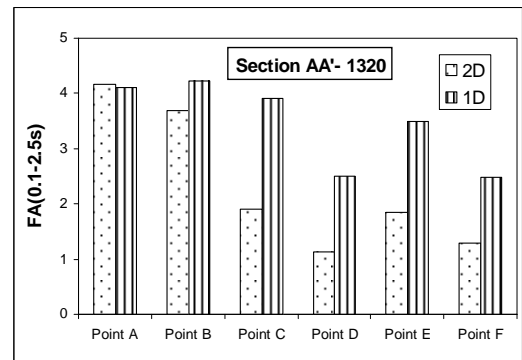


Fig. 10c. Amplification factors corresponding to 6 surficial points on section AA' for 1320 input motion.

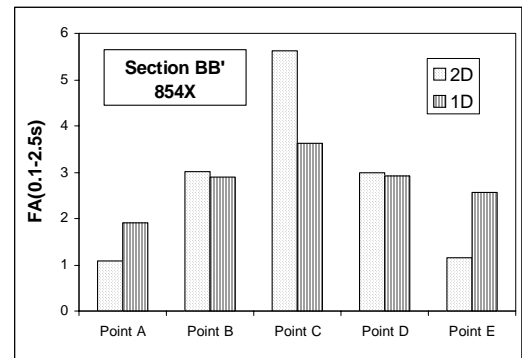


Fig. 11a. Amplification factors corresponding to 6 surficial points on section BB' for 854X input motion.

From Figs. 10-11 the magnitude of 2D and 1D amplification factors vary according to the input motion and the point considered. A general trend along the two sections shows 2D amplification factors result in lower amplification factor than

1D. This means that the geometrical irregularities in subsurface layer boundaries induce a reduction in 1D amplification factors which accounts for the impedance contrast between layers and their thicknesses.

Section AA' (Figs. 10a-c) shows the highest values 4.5 at node B for 854X and 642Y and 4.0 at node A for 1320 input motion.

In section BB' (Figs. 11a-c) where 2D amplification is more relevant than section AA', the large peak values at node C vary from 4 for the 854X input motion to 6 for the 642Y input motion. Seismic input motion 1320 induces a large deamplification at surficial nodes. The most severe input motion is 854X for section AA' and 642Y for section BB'.

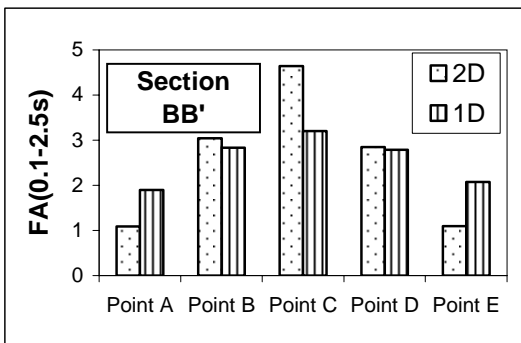


Fig. 11b. Amplification factors corresponding to 6 surficial points on section BB' for 642Y input motion.

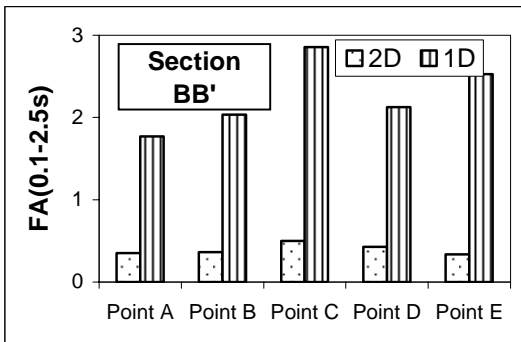


Fig. 11c. Amplification factors corresponding to 6 surficial points on section BB' for 1320 input motion.

Topographic amplification factors have been calculated according to Bouckovalas' equation (Fig. 12a-c and Fig. 13a-c) for sections AA' and BB'. In the case of section BB', such factor takes into account the valley effects instead of topographic ones. Bouckovalas defines values for two periods: $T = 0.2$ s and $T = 0.4$ s. Those were under and over the unity for the input motions and the period considered.

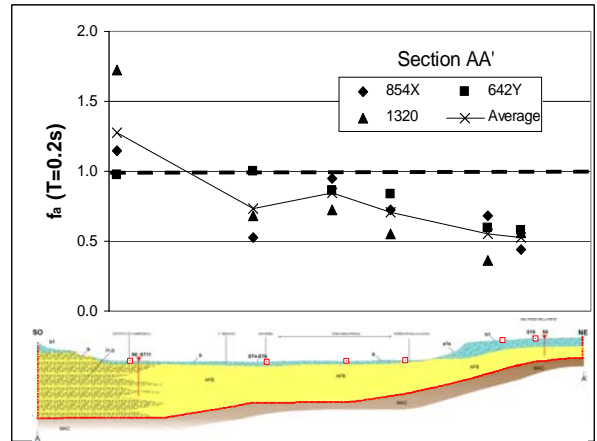


Fig. 12a. Topographic amplification factor for $T=0.2$ s at surficial nodes on section AA' and its mean trend.

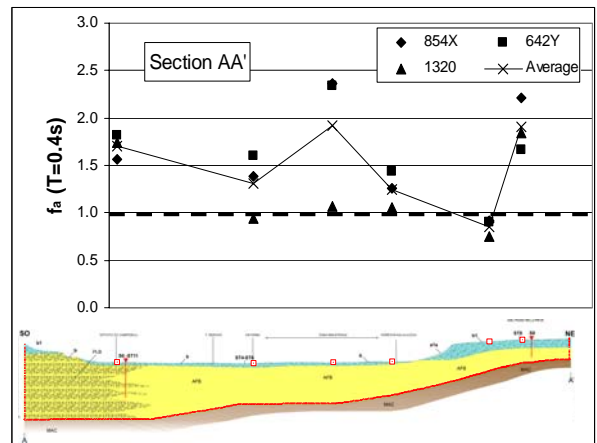


Fig. 12b. Topographic amplification factor for $T=0.4$ s at surficial nodes on section AA' and its mean trend.

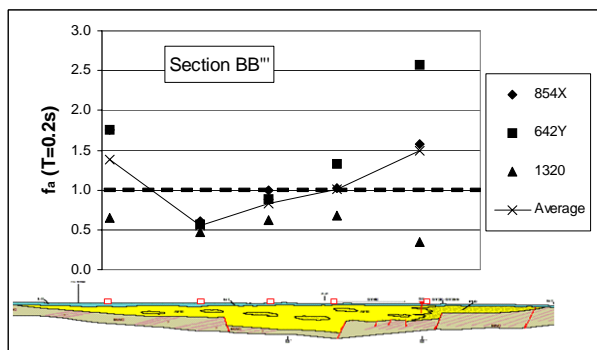


Fig. 13a. Topographic amplification factor for $T=0.2$ s at surficial nodes on section BB' and its mean trend.

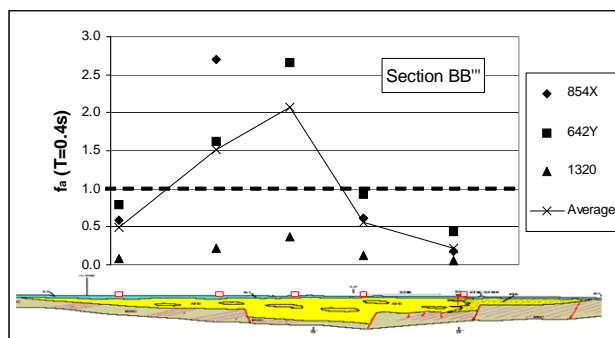


Fig. 13b. Topographic amplification factor for $T=0.4s$ at surficial nodes on section AA' and its mean trend.

The amplification factor f_a in section AA' at node A is equal to 1.2 and 1.7 at $T = 0.2$ s for input motions 854X and 1320 respectively. The topographic amplification effect at $T = 0.4$ s is evident at all the nodes but the node E which is the nearest point to a slope steeper than 15° . With respect to section BB', f_a values according to Eq. (6) are greater than 1 for nodes A and E at $T = 0.2$ s and for B and C at $T = 0.4$ s. As in section AA', f_a is lower than 1 for all nodes in section BB' for the input motion 1320.

This means topographic amplification cannot be used to define a unique value for each point because topographic amplification factors depend both on periods and on input motion frequency content and shape.

Discussion on results

Remarks on Eurocode 8. According to Eurocode 8, stratigraphic amplification effects depend on seismic soil category defined by the V_{S30} parameter, and topographic amplification effect depends on the angle of slope.

Table 12. Seismic amplification effects at surficial nodes on section AA'.

SECTION AA'						
Point	A	B	C	D	E	F
$f_a(T=0.2s)$	1.3	0.7	0.8	0.7	0.5	0.5
$f_a(T=0.4s)$	1.7	1.3	1.9	1.3	0.9	1.9

Table 13. Seismic amplification effects at surficial nodes on section BB'.

SECTION BB'					
Point	A	B	C	D	E
$f_a(T=0.2s)$	1.4	0.5	0.8	1.0	1.5
$f_a(T=0.4s)$	0.5	1.5	0.8	1.0	1.5

This means that for section AA' in Castelnuovo Garfagnana urban centre, the stratigraphic effects should be equal to 1.2 for B soils and 1.15 for C soils. At node E from section AA', the topographic amplification factor should be considered and the total amplification factor will be 1.38.

The highest geometrical amplification value is (Figs. 15-16) equal to 3.0, and is not considered because it is but one node of response for each section at one period.

Eqs. (7) is multiplied by S_S factor (Tab. 11) to define a new Type 1 acceleration spectrum as Eurocode 8 suggests. Figure 17 seems to be more reliable than the original Type 1 spectrum because, in this case, the geometrical amplification effect has been taken into account at all nodes.

Topographic slopes as well as buried irregular geometries should be taken into account in seismic local amplification effects but its contribution will not always be higher than 1. It depends on a complex combination of variables which add up to the geometry.

The geometric factor is strongly affected by input motion features. As this study shows the amplification effects for the same geometrical and geotechnical conditions depend on the energy content of the input accelerograms even though the spectrum compatibility is satisfied and the maximum acceleration is taken constant. As a matter of fact, 642Y and 854X accelerograms result in high amplification effects whereas 1320 accelerogram does not.

This occurrence can be associated with the Arias intensity of the three accelerograms. A Fig. 8 shows, 642Y and 854X accelerograms have higher Arias intensity (2 and 3 times respectively) than 1320. Further investigations should be carried out on this relationship.

Geometrical amplification factor. A geometrical amplification factor has been defined, according to Eq. (6) over the range 0.1s to 2.5s. This new factor takes into account both surficial and buried geometrical irregularities and the amplification variation over periods. As Fig. 14 shows at node E from section AA', geometrical amplification strongly varies over the period range. The highest amplification value is 1.7 at 0.6s. This occurs for the input motions 854X and 642Y whereas for the input motion 1320 the topographic factor calculated over the range 0.1-2.5s is always less than 1. Node E is the only one near a slope steeper than 15° so that both geometrical effects (topographic and buried) can be investigated.

The figure shows that for the most of the periods the geometrical factor is lower than 1 for all of the input motion considered.

Moreover, from the three geometrical factors calculated for the period range 0.1 s to 2.5 s, a mean value for each period can be determined instead of three values for the three input motions.

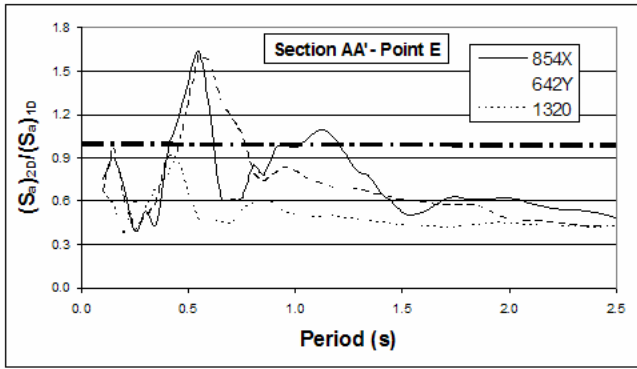


Fig. 14. Topographic factor calculated for the three input motion at node E on section AA'.

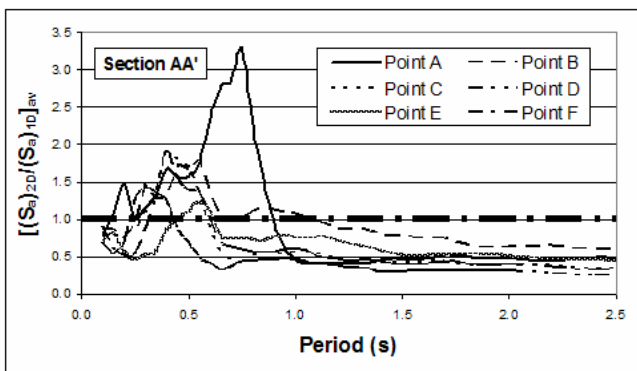


Fig. 15. Geometrical factors calculated over the range of periods 0.1 ÷ 2.5s at all surficial point in section AA'.

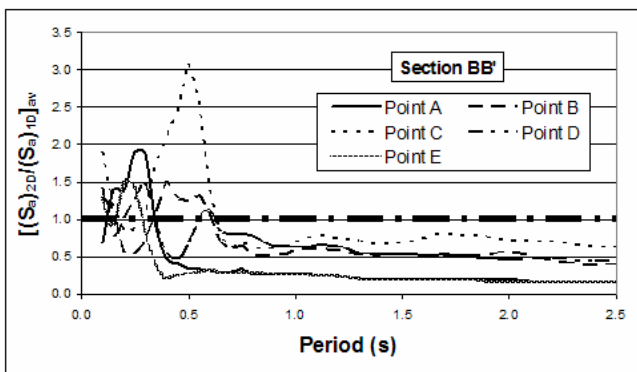


Fig. 16. Geometrical factors calculated over the range of periods 0.1 ÷ 2.5s at all surficial point in section BB'.

Figs. 15-16 show that different geometrical amplification effects occur at points corresponding to a flat topography and these values can be higher than for a slope (see node E in section AA' (Fig. 15)).

Those results provide more complete information on geometrical amplification effect than the topographic factor as

defined by Bouckovalas et al. (1999). A different approach to the topographic effect was define from of geometrical amplification functions than were defined as spectrum shaped function suggested by Eurocode 8.

For the case of Castelnuovo Garfagnana site, the following geometrical amplification function were defined:

$$\begin{aligned}
 0 \leq T \leq T_B &: S_g(T) = 20T \quad T_B = 0.1s \\
 T_B \leq T \leq T_C &: S_g(T) = 2 \quad T_C = 0.7s \\
 T_C \leq T \leq T_D &: S_g(T) = 4.3 - 3.3T \quad T_D = 1.0s \\
 T \geq T_D &: S_g(T) = 1.0
 \end{aligned} \quad (7)$$

The highest geometrical amplification value is (Figs. 15-16) equal to 3.0 and is not considered because it was but one node response for each section at one period.

The Eqs. (7) was multiplied by S_s factor (Tab. 11) to define a new Type 1 acceleration spectrum as Eurocode 8 suggests. Figure 17 seems to be more reliable than the original Type 1 spectrum because, in this case, the geometrical amplification effect has been taken into account at all nodes.

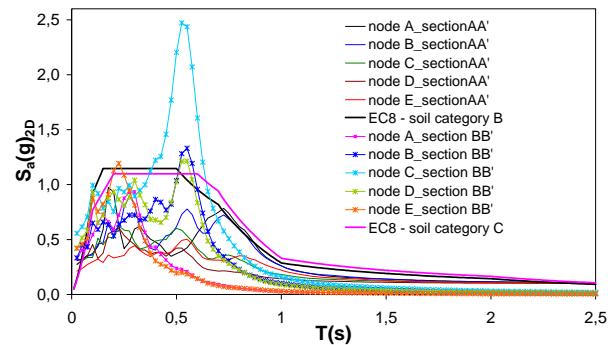


Fig. 17. Response spectra from 2D numerical analyses in sections AA' and BB' and EC8 spectra for soil categories B and C modified by geometrical amplification function.

CONCLUSIONS

Recent studies on local site effects have been carried out in Castelnuovo Garfagnana urban centre by means of 2D and 1D numerical simulations. From results two main observation were made:

- 1) The geometrical amplification effects on surficial flat geometries against the topographic amplification factor;
- 2) The relationship among input motion features, geometrical and stratigraphic amplifications.

Finally, the geometrical amplification function for the investigated site has been proposed. This function should be in order to be multiplied by the elastic response spectrum Type 1

(horizontal component) from Eurocode 8 for B and C soil categories.

Few considerations have been reported on the influence of the Arias intensity of input motions on site amplification effects. This issue needs further studies.

REFERENCES

Bouckovalas, G.D., G. Gazetas and A.G. Papadimitriou [1999], "Geotechnical aspects of the 1995 Aegion Greece, earthquake", *Proc. 2nd International Conference on Earthquake Geotechnical Engineering*, Lisboa, Balkema, 2, pp. 739-748.

Cancelli, A., G. D'Amato Avanzi, A. Pochini and A. Puccinelli [2002]. "Caratterizzazione geologica e litologico-tecnica delle pianure del Serchio e della Turrice Secca in prossimità di Castelnuovo Garfagnana (Lucca)", *Rivista Italiana di Geotecnica*, No. 3, pp. 17-32.

Crespellani, T., R. Bardotti, J. Facciorusso, C. Madiati and G. Vanucchi [2002]. "Studio geotecnico finalizzato alla valutazione degli effetti locali in alcuni siti campione della Garfagnana (Castelnuovo G., Pieve Fosciana, S. Romano G., Piazza al Serchio)", *Rivista Italiana di Geotecnica*.

Crespellani, T., J. Facciorusso, C. Madiati and G. Vanucchi [2002]. "Programma e controllo delle indagini geotecniche negli studi di microzonazione sismica a scala regionale: il caso della Garfagnana", *Rivista Italiana di Geotecnica*, No. 2, pp. 66-97.

Ferrini, M., M. Petrini V., D. Lo Presti, I. Puci, L. Luzi, F. Pergalani and Signanini P. [2001], "Numerical modelling for the evaluation of seismic response at Castelnuovo Garfagnana in Central Italy," *Proceedings of the 15th Int. Conf. on Soil Mech. and Geot. Eng.*, Turkey, Istanbul.

Final draft prEN 1998-1 [2003]. "*Eurocode 8: design of structures for earthquake resistance – Part. 1: general rules, seismic actions and rules for building*". CEN.

Foti, S., D. Lo Presti, O. Pallata, M.L. Rainone and P. Signanini [2002]. "Indagini geotecniche e geofisiche per la caratterizzazione del sito di Castelnuovo Garfagnana (Lucca)", *Rivista Italiana di Geotecnica*, No. 3, pp. 42-60.

Geo-slope International [2004]. "*GeoStudio. Suite software che integra tutti i prodotti Geo-Slope in un unico ambiente di lavoro*". ADALTA - software per la scienza ed il business.

Housner G.W. [1952], "Spectrum intensities of strong motion earthquakes", *Proc. Of the Symposium on Earthquakes and Blast effects on Structures*, Earth. Eng. Res. Inst.

Hudson, M., I.M. Idriss, M. Beikae [1994]. "*Quad4M. A computer program to evaluate the seismic response of soil*

structures using finite element procedures and incorporating a compliant base". User's manual CGM, Davis, California.

Idriss, I.M. and J.I. Sun [1992]. "*Shake91. A computer program for conducting equivalent linear seismic response analysis of horizontally layered soil deposits*". University of California, Berkeley

Lai, C., C. Strobbia and Dall'Ara G. [2005]. "*Elaborazione di Raccomandazioni e di linee guida per la definizione dell'input sismico e delle modellazioni da adottare nei territori della regione Toscana nell'ambito del progetto di ricerca "VEL" ai sensi della nuova normativa sismica (Ordinanza PCM n°3274 del 20/3/2003 e successivi aggiornamenti) – Parte 1 – Definizione dell'input sismico*". Eucenter technical report.

Lo Presti, D., C.G. Lai, A. Camelliti and T.O. Crespellani [2000], "Analisi non lineare della risposta sismica dei terreni", *Atti Convegno GeoBen 2000, Geological and geotechnical influences in the preservation of historical and cultural heritage*, Torino, pp. 601-612.

Lo Presti D., C.G. Lai, A. Camelliti and I. Puci [2001], "Onda: un Codice di Calcolo per l'Analisi Non-Lineare della Risposta Sismica dei Terreni", *Tema 10, IARG*, Milano.

Lo Presti, D., L. Luzi, F. Pergalani, V. Petrini, I. Puci and P. Signanini [2002]. "Determinazione della risposta sismica dei terreni a Castelnuovo Garfagnana (Lucca)", *Rivista Italiana di Geotecnica*, No. 3, pp. 61-74.

Ministero delle Infrastrutture e dei trasporti [2005]. *Norme Tecniche per le Costruzioni*.

Nardi, R., A. Puccinelli and P.L. De Lucia [1986]. "*Carta geologica e carta della franosità della Garfagnana e della Media Valle del Serchio (Lucca) in scala 1:10.000. Elemento "Castelnuovo di Garfagnana" (scala 1:10.000)*". Tipografia SELCA, Firenze.

Ordinanza del Presidente del Consiglio dei Ministri n. 3274 del 20 marzo 2003 [2003]. "*Primi elementi in materia di criteri generali per la classificazione sismica del territorio nazionale e di normative tecniche per le costruzioni in zona sismica*". G.U. n. 72.

Pergalani, F., R. Romeo, L. Luzi, V. Petrini, A. Pugliese and T. Sano [1999]. "Seismic microzoning of the area struck by Umbria-Marche (Central Italy) Ms 5.9 earthquake of 26 September 1997", *Soil Dynamics and Earthquake Engineering*, No. 18, pp. 279-296.

Petrini, V. [1998]. "*Determinazione del rischio sismico a fini urbanistici dei comuni di Minacciano, piazza al Serchio, San Romano in Garfagnana e Castelnuovo Garfagnana*". Rapporto interno, Dipartimento delle Politiche Territoriali, Regione Toscana.